

The distribution of maximum ice scour sizes by sea depth at the seabed of the Barents and Kara Seas

Osip Kokin^{1,2}, Stepan Maznev^{1,2,4}, Vasily Arkhipov^{1,2}, Evgeniy Moroz¹, Elena Sukhikh¹, Roman Ananiev³, Sergey Nikiforov³, Nikolay Sorokhtin³, Sergey Vernyaev⁴

¹ Geological Institute of Russian Academy of Sciences (Moscow, Russia)

² Lomonosov Moscow State University (Moscow, Russia)

³ Shirshov Institute of Oceanology of Russian Academy of Sciences (Moscow, Russia)

⁴ ICEMAN.KZ LLP (Almaty, Kazakhstan)

ABSTRACT

Ice scouring is very important process in terms of impact assessment on underwater engineering structures. In this work, we present new data of last years obtained during recent cruises of research vessels in comparison with the generalized previously published data on the distribution of ice scours on the seabed of the Barents and Kara Seas. All collected data were combined into a database of maximum ice scour sizes. According to the database, graphs of the sea depth distribution of the maximum ice scour depth and width were plotted. Analysis of these graphs showed that they: reflect a history of relative sea level changes; make it possible to estimate the magnitude of the change in relative sea level and the maximum size of iceberg keels at certain sea levels; provide additional indirect evidence for the ice scour age, complement the understanding of the ice scour division into modern and relict ones (in addition to the currently widely used bathymetric approach); make it possible to estimate the theoretically possible maximum size of “normal” ice scours for a given sea depth in the presence of an iceberg with a keel corresponding to the sea depth.

KEY WORDS: Icebergs; Seabed topography; Ice effects; Ice gouging.

INTRODUCTION

Ice scouring (or ice gouging) is a process of interaction of sea ice or icebergs with the seabed. It is associated with the origin of landforms named ice scours (or ice-keel scours, or ice gouges, or ice ploughmarks). This process is very important in terms of impact assessment on underwater engineering structures (e.g., pipelines). Icebergs being critical features that affect both marine operations and the design of structures are understudied in the Barents-Kara region. A large number of researches were conducted on the ice scours in the Barents Sea, and plenty of them was published. There are much less published data on the Kara Sea ice scours. Unfortunately, there is little knowledge available on spatial distribution. In this work, we present new data obtained during cruises of research vessels in last years in comparison

with the generalized previously published data on the distribution of ice scours on the seabed of the Barents and Kara Seas (Maznev, et al., 2023). The goal of this work is to assess the distribution of the maximum ice scour sizes by sea depth in the Barents-Kara region.

MATERIALS AND METHODS

Regional Settings

The Barents and Kara Seas belong to the western part of the Russian Arctic. Glaciers descending into the sea account for about a quarter of the Barents Sea coast. Svalbard, Franz Joseph Land (FJL), and Novaya Zemlya produce the majority of iceberg calving in the Russian Arctic. The depths within Barents Sea do not exceed 600 m, averaging ~200–250 m. In the central and northern parts of the sea, a number of banks with depths of up to 50–100 m is located, as well as troughs with depths of up to 500–600 m. The lack of riverine material supply defines a low sedimentation rate. The heat of the North Cape Current penetrating from the Atlantic Ocean leads to scarce ice on the Barents Sea. Fast ice is poorly developed and favors iceberg drift.

The Kara Sea is characterized by average depths of 50–100 m with a maximum of just more than 600 m in troughs. The Novaya Zemlya Trough, with depths up to 450 m, extends along Novaya Zemlya; to the north of it is the St. Anna Trough, with depths up to 620 m. In the northern part of the sea the Central Kara Plateau has depths of 70–250 m and the Voronin Trough is deeper than 270 m. In comparison to the Barents, the Kara Sea receives a significant amount of sedimentary material in runoff from the rivers, as well as from coastal erosion due to thermal abrasion of permafrost. Novaya Zemlya limits the penetration of warm water masses from the west considerably. Fast ice occupies a significant area.

During the Pleistocene, in the Barents–Kara region ice sheets formed on the shelf and in large archipelagos (Svendsen, et al., 2004). During the Last Glacial Maximum (LGM, MIS 2, about 20 ka BP) the Scandinavian Mountains, Svalbard, FJL, and Novaya Zemlya were the centers of glaciation and ice supply. Glaciation centers also possibly existed on the Kara and Barents shelves. The global (eustatic) ocean level during the LGM was about 120 m lower (Waelbroeck, et al., 2002). However, relative sea level is additionally determined by glacioisostatic and neotectonic land movements. Due to this, there is an opinion that about 12 ka BP (Younger Dryas), the depth of the Barents Sea exceeded the modern one by 50–150 m (Patton, et al., 2017). By this time, the global sea level had risen by 60 m and was 60 m lower than present-day (Waelbroeck, et al., 2002), while the ice sheets reduced practically to the present-day size. Then, during the Holocene, the global sea level gradually rose until it reached the present level of about 5 ka BP (Dittmers, et al., 2008). At that time, a compensatory glacioisostatic uplift of the lithosphere took place over most of the Barents Sea shelf, causing a drop in the relative sea level, since the rate of glacioisostatic uplift exceeded the eustatic sea level rise. At the same time, the southeastern Barents Sea and most of the Kara Sea did not have a compensatory rise, so the relative sea level here probably rose continuously, as did the global average (Baranskaya, et al., 2018).

Data sources

In this paper, we use two main types of data source: (1) our own multibeam seabed survey during research vessels (R/V) cruises in the last years and (2) published data. The survey data is presented in two ways. They are: the areal survey (series of parallel survey lines),

providing detailed seabed digital elevation models (DEMs) on a certain, specially selected (rarely for ice-scouring studies) small areas (polygons), and transit survey between polygons (single survey line) that produces a narrow but long-distance DEM band at a random seabed location. Thus, we distinguish three types of data coverage from which ice scour populations have been established:

- polygons – detailed DEMs (mostly our own but also published) from a certain small area (discrete data);
- segments – our own DEMs from transit surveys divided into depth intervals (continuous data);
- areas – data from published sources, as usual providing general unspecified knowledge attached to large areas.

Multibeam seabed survey

Multibeam seabed survey was carried out on cruises of the Shirshov Institute of Oceanology RAS: cruise 52 of the R/V Akademik Nikolaj Strakhov (ANS-52, 2021) and cruise 51 of the R/V Akademik Boris Petrov (ABP-51, 2022). Based on the data of ANS-52 cruise, transit survey lines (segments) were studied, and according to the data of ABP-51 cruise, polygons were studied. The results of the polygons study in the ABP-51 cruise have already been partially published (Kokin, et al., 2022).

The main equipment of the seabed mapping marine hydroacoustic by RESON used for multibeam survey during the ANS-52 cruise was:

- the software and hardware system SeaBat with multibeam echosounders SeaBat 8111 (shallow) and SeaBat 7150 (deep);
- GPS motion sensors and gyrocompass combined in the Applanix POS-MV device;
- sound speed sensor for SVP-70 echo sounder antennas.

The SeaBat 7150 deep-sea multibeam modular echosounder has a 12 kHz frequency and up to 150° coverage. The SeaBat 8111 is a high-resolution 100 kHz multi-beam echosounder with the same coverage.

Data acquired from these echosounders was collected and processed in PDS2000 software with the creation of seabed DEMs to further estimate the maximum depth and width of the ice scours within a polygons or segments.

RESULTS

The spatial distribution of the ice scour population (polygons, segments and areas) for which estimations of the maximum ice scour depth and width in the Barents and Kara Seas have been made are shown in Figure 1.

All collected data were combined into a database of maximum ice scour sizes at the seabed of the Barents and Kara Seas (Table 1). The database includes the following features:

- N – number of ice scour populations shown in the Figure 1;
- Type – type of data coverage from which ice scour populations have been established: polygons (P), segments (S), and areas (A);
- SD – sea depth range of ice scour population, m;

- MSD – mean sea depth of ice scour population, m;
- MISD – maximum ice scour depth, m;
- MISW – maximum ice scour width, m.

In addition, for each ice scour population, the source of data is indicated:

- in the Barents Sea: 1, 3-4 (Moroz, 2017); 2 (Solheim, 1997); 3, 5-6 (Zaionchek, et al., 2010); 7-8, 10-11, 16 (Bjarnadottir, et al., 2014); 7 (Solheim, et al., 1988); 9, 12-13, 15 (Newton, et al., 2017); 11, 20, 26 (Mironyuk, et al., 2018a); 14 (Vadakkepuliymbatta, et al., 2016); 14 (Chand, et al., 2016); 14 (Thorsnes, et al., 2016); 17 (Moroz, et al., 2020); 18 (Razuvaeva, et al., 2007); 19-21, 26 (Mironyuk, et al., 2018b); 22 (Polyak, et al., 1997); 23-25 (Kokin, et al., 2022); 24-25 (Denisova, et al., 2022);
- in the Kara Sea: 27 (Aksenov, et al., 2022); 28 (Tokarev, et al., 2022); 29-30, 32, 35-36, 47, 54, 56, 65-66, 68 (Kokin, et al., 2022); 31 (Pronin, et al., 2016); 33 (Rybalko et al., 2020); 34 (Zamotina, et al., 2022); 37-46, 48-53, 55, 57-64, 67 (this paper).

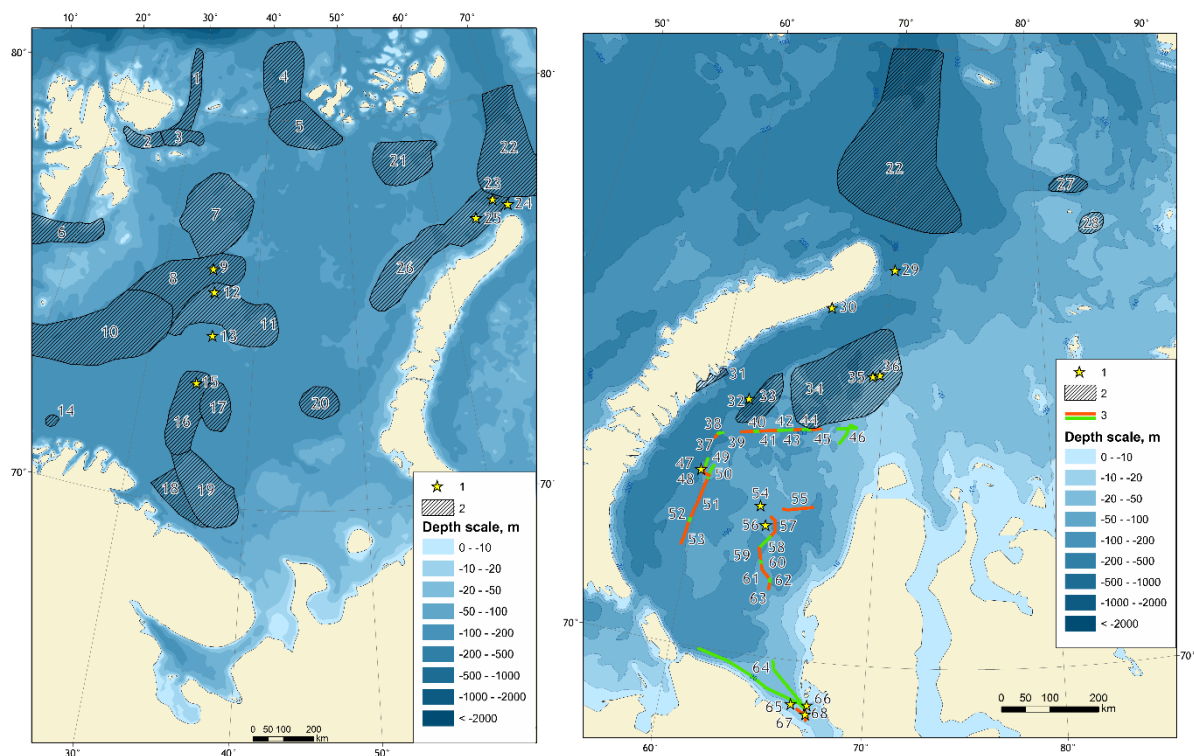


Figure 1. The spatial distribution of the ice scour populations in the Barents (left) and Kara (right) Seas: 1 – polygons, 2 – areas, and 3 – segments.

According to the database (Table 1), graphs of the sea depth distribution of the maximum ice scour depth and width in the Barents and Kara Seas were plotted (Figures 2 and 3). Each point on the graph corresponds to one ice scour population shown in Figure 1. We can see that in the Barents and Kara Seas, the depth distribution of the maximum ice scour sizes has a different pattern. The analyzed ice scour populations are located in the sea depth range of 90-480 m in the Barents Sea and 15-300 m in the Kara Sea. The maximum ice scour depth varies from 2 to 20 m in the Barents Sea and from 0,2 to 9,4 m in the Kara Sea, and the maximum ice scour width varies from 25 to 500 m in the Barents Sea (one case of 800 m we consider erroneous) and from 10 to 300 m in the Kara Sea. There is no clear correlation between ice

scour size and sea depth. However, it can be seen that many points form chains along several oblique imaginary lines subparallel to each other.

Table 1. A database of maximum ice scour sizes at the seabed of the Barents and Kara Seas.

Barents Sea						Kara Sea					
Z	Type	SD	MSD	MISD	MISW	Z	Type	SD	MSD	MISD	MISW
1	A	130-140	135	7	-	27	A	70-150	110	-	-
2	A	85-100	93	8	25	28	A	30-50?	40	-	-
3	A	110-130	120	5	800	29	P	80-110	95	5	110
		100-200	150	5	-			170-185	178	5,4	50
4	A	350-370	360	-	-	30	P	68-110	89	3,6	40
5	A	250-350	300	8	40	31	A	25-65	45	-	-
6	A	280-350	315	-	-	32	P	250-275	263	3,5	180
7	A	150-170	160	6	250	33	A	130-340	235	8	300
		170-210	190	12	110	34	A	30-50	40	-	-
8	A	180-340	260	7	400	35	P	37-39	38	3	60
9	P	220-230	225	8	125	36	P	33-38	35,5	0,2	50
10	A	230-250	240	20	500	37	S	280-320	300	4,6	102
		320-340	330	20	500	38	S	240-280	260	3	80
		380-440	410	4	300	39	S	140-180	160	7	72
		470-490	480	20	500	40	S	80-140	110	3,2	70
11	A	190-250	220	5	400	41	S	100-140	120	6,3	66
		240-250	245	6	60	42	S	160-200	180	3,5	89
12	P	180-190	185	10	250	43	S	100-140	120	3,7	98
13	P	180-210	195	10	500	44	S	140-180	160	6,1	171
14	A	310-350	330	12	150	45	S	80-140	110	3,5	101
		330-390	360	7	125	46	S	20-60	40	4	68
		420-440	430	12	250	47	P	130-180	155	3	60
15	P	200-300	250	3	70	48	S	100-160	130	9,4	182
		270-280	275	5	50	49	S	140-220	180	6	92
16	A	170-260	215	10	200	50	S	60-100	80	7,3	153
17	A	190-330	260	9	250	51	S	100-140	120	4,8	208
18	A	185-230	208	5	300	52	S	80-100	90	4,2	118
19	A	120-195	158	15	240	53	S	100-140	120	3,6	179
20	A	300-320	310	16	300	54	P	47-50	48,5	0,8	25
		320-340	330	3	100	55	S	60-100	80	2,8	148
21	A	70-200	135	15	60	56	P	80-95	87,5	2	100
22	A	300-550	425	20	200	57	S	60-140	100	2,9	75
23	P	250-280	265	10	420	58	S	100-140	120	2,1	101
		300-310	305	8	450	59	S	80-100	90	3,5	120
24	P	225-235	230	5,5	80	60	S	100-140	120	3,2	66
		320-345	333	10	260	61	S	60-100	80	4,6	130
		260-300?	280	5	190	62	S	100-120	110	2,7	104
25	P	95-110	103	2,5	130	63	S	80-100	90	1,5	58
		90-120	105	2	95	64	S	20-40	30	2,5	49
26	A	95-140	118	10	100	65	P	22-24	23	0,4	10
		320-380	350	20	200	66	P	21-24	22	0,8	100
						67	S	10-20	15	2,3	55
						68	P	23-24	23,5	1,2	70

DISCUSSION

The lack of a clear correlation between ice scour size and sea depth, as well as the concentration of points along several subparallel imaginary lines, inclined in the direction of

increasing ice scour size with sea depth, can be associated with the following points:

- linear relationship between the ice-keel size and the ice scour size: the larger ice-keel (the greater the seabed depth at which the contact of ice with the seabed occurs), the greater the size of the traces left (the depth and width of the ice scours);
- the formation of ice scours currently observed on the seabed occurred at different sea levels.

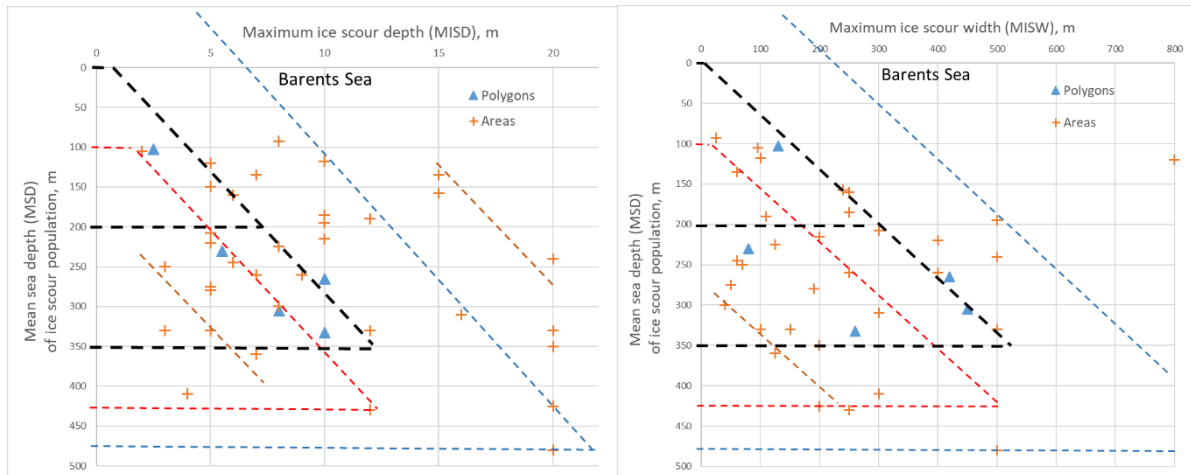


Figure 2. The sea depth distribution of the maximum ice scour depth (left) and width (right) in the Barents Sea.

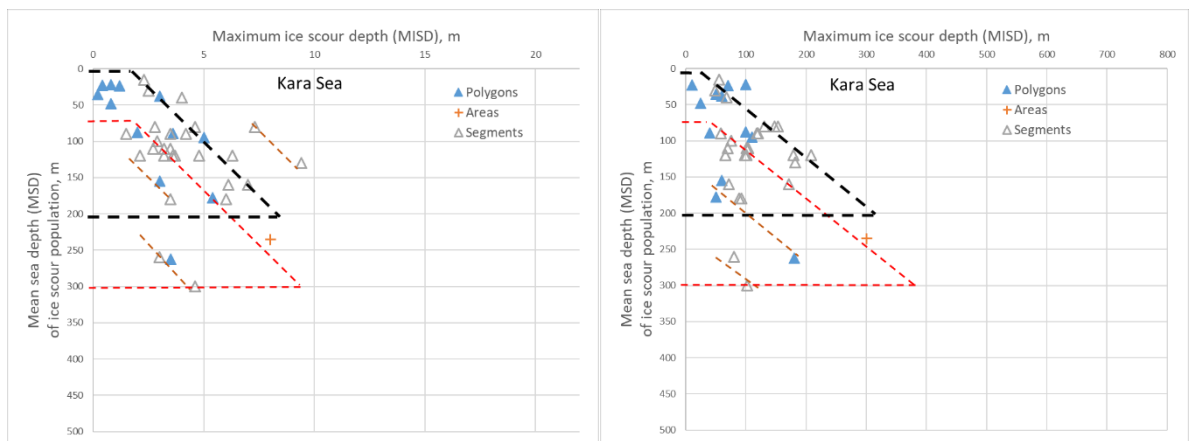


Figure 3. The sea depth distribution of the maximum ice scour depth (left) and width (right) in the Kara Sea.

Therefore, on the graphs of maximum ice scour size distribution by sea depth, instead of one trend line, several trend lines can be observed. Thus, on the graphs, one can distinguish the “limit” lines of the dependence of the ice scour sizes on the ice-keels sizes (i.e., the sea depth of the ice scours), which represent the limit “above” which ice scour cannot form for a given size of the ice-keel (ice scour sea depth). In other words, for a particular sea level, the points on the graph should always be located either under or on the “limit” line that limits them from above. Theoretically, there should be no points above the “limit” line. However, the influence of other factors (for example, the composition of sediments) on the abnormally large ice scours formation cannot be ruled out.

When the sea level changes, the “limit” lines are shifted after it. It is clear that the area of points under the "limit" line of one sea level may intersect with the area of points under the "limit" line of another sea level. The location of the "limit" lines at other sea levels is determined by the high density of points along an oblique imaginary line and the history of changes in relative sea level.

The graphs show the following supposed “limit” lines:

- black dotted line is related to present sea level;
- red dotted line is related to a relative sea level below the present;
- blue dotted line is related to a relative sea level above the present.

The orange dotted line shows the lines corresponding to the chains of dots below and parallel to the “limit” lines. They probably mark some "specific limit" lines (for example, the “regional limit” line in the East Novaya Zemlya Trench at a sea depth of more than 250 m).

2-3 horizontal lines (1 upper and 1-2 lower) are added to the “limit” lines, limiting the depths range in which this “limit” line supposedly “works”. The upper horizontal line corresponds to the sea level for which the “limit” line is assumed. The lower horizontal line corresponds to the assumed maximum sizes of iceberg keels for the given “limit” line and sea level. The 2 lower horizontal lines in the Barents Sea suggest 2 variants of keel sizes: up to 200 m (modern icebergs) and up to 350 m (palaeoicebergs of a more severe climate than modern, but at modern sea level). The allocation of the 2nd horizontal line (350 m) was due to the fact that the points of the graph continue up to 350 m.

Thus, the “limit” " and horizontal lines define some "trapezoids" (or almost "triangles" as, for example, in the Barents Sea) containing certain areas of points. These trapezoids (or triangles) determine at what depths and what sizes ice scours are formed at a certain relative sea level, which corresponds to the top of each trapezoid (or triangle).

CONCLUSIONS

The distribution of maximum ice scour sizes by sea depth in a water basin:

- reflects a history of relative sea level changes;
- makes it possible to estimate the magnitude of the change in relative sea level and the maximum size of iceberg keels at certain sea levels;
- provides additional indirect evidence for the ice scour age, complement the understanding of the ice scour division into modern and relict ones (in addition to the currently widely used bathymetric approach);
- makes it possible to estimate the theoretically possible maximum size of “normal” ice scours for a given sea depth in the presence of an iceberg with a keel corresponding to the sea depth.

Plotted graphs for the Barents Sea based primarily on published data are less accurate than plotted graphs for the Kara Sea based primarily on field data. Plotted graphs for the ice scour depth are less accurate than plotted graphs for the ice scour width due to the more difficult unambiguous estimation of ice scour depth.

For the Barents Sea, 3 main sea levels can be tentatively identified at which the ice scours were formed: 1) the current sea level; 2) the sea level is about 100 m lower than the current one; 3) the sea level is about 150-170 m higher than the current one. For the Kara Sea, 2 main

sea levels are distinguished, at which ice scours were formed: 1) the current sea level; 2) the sea level is about 70-80 m lower than the current one.

During the climate cooling of the last 5 kyr, at the current sea level, in the Barents Sea, the maximum size of iceberg keels could reach 350 m. At the same time, in the Kara Sea, the maximum size of iceberg keels did not exceed 200 m.

In the Barents Sea, the maximum size of iceberg keels at a relative sea level about 100 m lower than the current one (about 330 m) was similar to such size during the cooling of the last 5 kyr, and was almost 2 times larger (about 650 m) at a relative sea level about 150-170 m higher than the current one. In the Kara Sea, the maximum size of iceberg keels was close to those for the last 5 kyr (about 220 m) at a relative sea level about 70–80 m lower than the current one.

The plotted graphs show that the boundary between modern and relict ice scours is not sharp (as, for example, the 200 m isobath), their distribution areas can intersect. The anomalous size of the ice scour for a given sea depth may indicate ice scour relict age (formation at a relative sea level above the present). Therefore, in the Barents Sea, relict ice scours can occur even at sea depths of up to 200 m. It is assumed that among the analyzed populations of ice scours in the Barents Sea, relict ice scours predominate, and in the Kara Sea, ice scours formed at present sea level predominate. In addition to the history of changes in the relative sea level, this is due to the peculiarities of the distribution of sea depths relative to the maximum sizes of iceberg keels.

Based on the concept of the maximum possible keel size of a modern iceberg in the Barents-Kara region no more than 200 m, we can assume that the largest modern “normal” ice scour cannot exceed about 7-8 m deep and about 300 m wide.

The obtained quantitative estimates are preliminary and require clarification as new data become available.

ACKNOWLEDGEMENTS

The work was funded by the Russian Science Foundation, project no. 21-77-20038, GIN RAS, <https://rscf.ru/en/project/21-77-20038>.

Acknowledgments to the cruise administration, crew and participants of the R/V *Akademik Nikolaj Strakhov* and R/V *Akademik Boris Petrov* for their support and assistance in organizing offshore activities and at sea during the cruises ANS-52 (2021) and ABP-51 (2022).

REFERENCES

- Aksenov, A.O., Rybalko, A.E., Pirogova, A.S., Kudinov, A.A., Dudkov, I.Yu., & Tokarev, M.Yu., 2022. A variety of bedforms in the eastern part of central Kara Trough (preliminary result of expedition TTR-21). In: Ed. Gusev E.A. Relief and Quaternary deposits of the Arctic, Subarctic and North-West Russia. *Proceedings of the annual conference on the results of expedition research*, 9, pp.15-19.
- Baranskaya, A.V., Khan, N.S., Romanenko, F.A. et al., 2018. A postglacial relative sea-level database for the Russian Arctic coast. *Quat. Sci. Rev.*, 199, pp.188-205.
- Bjarnadottir, L.R., Winsborrow, M.C.M., & Andreassen, K., 2014. Deglaciation of the central Barents Sea. *Quaternary Science Reviews*, 92, pp.208-226.

Chand, S., Thorsnes, T., Rise, L., Brunstad, H., & Stoddart, D., 2016. Pockmarks in the SW Barents Sea and their links with iceberg ploughmarks. In: Eds. Dowdeswell, J. A., Canals, M., Jakobsson, M., Todd, B. J., Dowdeswell, E. K. & Hogan, K. A. *Atlas of Submarine Glacial Landforms: Modern, Quaternary and Ancient*. Geological Society, London, Memoirs, 46, pp.295-296.

Denisova, A.P., Moroz, E.A., Eremenko, E.A., Sukhikh, E.A., & Arkhipov, V.V., 2022. Signs of degassing within the glacial shelf in the north-eastern part of the Barents Sea. In: Ed. Gusev E.A. Relief and Quaternary deposits of the Arctic, Subarctic and North-West Russia. *Proceedings of the annual conference on the results of expedition research*, 9, pp.78-86.

Dittmers, K.H., Niessen, F., & Stein, R., 2008. Acoustic facies on the inner Kara Sea Shelf: Implications for late Weichselian to Holocene sediment dynamics. *Mar. Geol.*, **254**(3-4), pp.197-215.

Jakobsson, M., Andreassen, K., Bjarnadottir, L.R. et al., 2014. Arctic Ocean glacial history. *Quat. Sci. Rev.*, 92, pp.40-67.

Kokin, O.V., Arkhipov, V.V., Meshcheryakov, N.I., Ananiev, R.A., Slukovsky, Z.I., & Sukhikh, E.A., 2022. The ice-gouging landforms investigation of the south-western part of Kara Sea and the north-eastern part of the Barents Sea in the 51st cruise of the R/V "Academik Boris Petrov". In: Ed. Gusev E.A. Relief and Quaternary deposits of the Arctic, Subarctic and North-West Russia. *Proceedings of the annual conference on the results of expedition research*, 9, pp.123-127.

Maznev, S.V., Kokin, O.V., Arkhipov, V.V., & Baranskaya A.V., 2023. Modern and relict evidence of iceberg scouring of the Barents and Kara seafloors. *Oceanology*, 63(1), pp.95-107.

Mironyuk, S.G., & Ivanova, A.A., 2018a. Micro- and mesorelief of the glacial shelf of the Western Arctic seas in the light of new data. *Bulletin of Quaternary Period Commission*, 76, pp.41-58.

Mironyuk, S.G., Ivanova, A.A., & Kolyubakin, A.A., 2018b. Extreme depths of modern ice gouging on the shelf of the northeastern part of the Barents Sea. *Russian Polar Studies*, 1, pp.12-14.

Moroz, E.A., 2017. *Neotectonics and bottom topography of the northwestern margin of the Barents Sea shelf and its framing*. Ph.D. Moscow: Geological Institute of the Russian Academy of Sciences.

Moroz, E.A., Zarajskaya, Yu.A., Sukhikh, E.A., Sokolov, S.Yu., Ermakov, A.V., & Abramova, A.S., 2020. Relief and structure of the upper part of sedimentary cover in the area of the Fedynsky rise according to acoustic data. *Vestnik Moskovskogo Unviersiteta, Seriya Geografiya*, 2, pp.82-91.

Newton, A.M.W., & Huuse, M., 2017. Glacial geomorphology of the central Barents Sea: Implications for the dynamic deglaciation of the Barents Sea Ice Sheet. *Marine Geology*, 387, pp.114-131.

Nikiforov, S.L., Sorokhtin, N.O., Ananiev, R.A., Dmitrevskiy, N.N., Moroz, E.A., & Kokin, O.V., 2022. Research in Barents and Kara Seas during cruise 52 of the R/V Akademik Nikolaj

Strakhov. *Oceanology*, 62(3), pp.433-434.

Patton, H., Hubbard, A., Andreassen, K. et al., 2017. Deglaciation of the Eurasian ice sheet complex. *Quat. Sci. Rev.*, 169, pp.148-172.

Polyak, L., Forman, S.L., Herlihy, F.A. Ivanov, G., & Krinitsky, P., 1997. Late Weichselian deglacial history of the Svyataya (Saint) Anna Trough, northern Kara Sea, Arctic Russia. *Marine Geology*, 143, pp.169-188.

Pronin, A.A., Rimskii-Korsakov, N.A., & Surin, M.N., 2016. Ice gouging in the Kara Sea recorded by side-scan sonar. In: *Proceedings of All-Russian Conference "Applied Technologies of Hydroacoustics and Hydrophysic*, 13, pp.414-415.

Razuvaeva, E.I., & Zinchenko, A.G., 2007 New data on the mesorelief of the bottom of the Kola Trench (Barents Sea). In: *Proceedings of XVII International Scientific Conference (School) on Marine Geology*, pp.155-157.

Rybalko, A.E., Mironyuk, S.G., Roslyakov, A.G., Kolyubakin, A.A., Solovjeva, M.A., Terekhina, Ya.E., & Tokarev, M.Yu., 2020. New signs of sheet glaciation in the Kara Sea: megascale glacial linearity in the East Novaya Zemlya Trough. In: Ed. Gusev E.A. Relief and Quaternary deposits of the Arctic, Subarctic and North-West Russia, *Proceedings of the annual conference on the results of expedition research*, 7, pp.175-181.

Solheim, A., 1997. Depth-Dependent Iceberg Plough Marks in the Barents Sea. In: *Glaciated Continental Margins*, Eds. Davies T.A. et al. Dordrecht: Springer, pp. 138–139.

Solheim, A., Milliman, J.D., & Elverhoi, A., 1988. Sediment distribution and sea-floor morphology of Storbanken: implications for the glacial history of the northern Barents Sea. *Canadian Journal of Earth Sciences*, 25(4), pp.547-556.

Svendsen, J.I., Alexanderson, H., Astakhov, V.I. et al., 2004. Late Quaternary ice sheet history of northern Eurasia. *Quat. Sci. Rev.*, 23, pp.1229-1271.

Thorsnes, T., Brunstad, H., Lågstad, P., & Chand, S., 2016. Trawl marks, iceberg ploughmarks and possible whale-feeding marks, Barents Sea. In: Eds. Dowdeswell, J. A., Canals, M., Jakobsson, M., Todd, B. J., Dowdeswell, E. K. & Hogan, K. A. *Atlas of Submarine Glacial Landforms: Modern, Quaternary and Ancient*. Geological Society, London, Memoirs, 46, pp.293-294.

Tokarev, M.Yu., Bulanova, I.A., Shindina, N.E., Tomasenko, S.V., Ugolkova, E.A., Pirogova, A.S., & Rybalko, A.E. Examples of the manifestation of cryogenic processes in the surroundings of Uedineniya Island (Kara Sea). In: Ed. Gusev E.A. Relief and Quaternary deposits of the Arctic, Subarctic and North-West Russia. *Proceedings of the annual conference on the results of expedition research*, 9, pp.258-261.

Vadakkepuliymbatta, S., Bünz, S., Tasiannas, A., & Mienert, J., 2016. Iceberg ploughmarks in the SW Barents Sea imaged using high-resolution P-Cable 3D seismic data. In: Eds. Dowdeswell, J. A., Canals, M., Jakobsson, M., Todd, B. J., Dowdeswell, E. K. & Hogan, K. A. *Atlas of Submarine Glacial Landforms: Modern, Quaternary and Ancient*. Geological Society, London, Memoirs, 46, pp.281-282.

Waelbroeck, C., Labeyrie, L., Michel, E. et al., 2002. Sea-level and deep water temperature

changes derived from benthic foraminifera isotopic records. *Quat. Sci. Rev.*, 21, pp.295-305.

Zaionchek, A.V., Brekke, H., Sokolov, S.Yu., Mazarovich, A.O., Dobrolyubova, K.O., Efimov, V.N., Abramova, A.S., Zarajskaya, Yu.A., Kohan, A.V., Moroz, E.A., Pejve, A.A., Chamov N.P., & Yampol'skij, K.P., 2010. Structure of the continent–ocean transition zone of the northwestern framing of the Barents Sea (according to the data of cruises 24–26 of the R/V Akademik Nikolai Strakhov, 2006–2009). In: *The Structure and History of the Development of the Lithosphere*, Ed. Leonov Yu.G. Moscow: Paulsen, pp.111-157.

Zamotina, Z.S., Terekhina, Ya.E., Rybalko, A.E., Repkina, T.Yu., & Kolubakin, A.A. Erosive-accumulative objects distribution landforms in the northern part of the Kara Sea East-Novaya Zemlya area. In: Ed. Gusev E.A. Relief and Quaternary deposits of the Arctic, Subarctic and North-West Russia. *Proceedings of the annual conference on the results of expedition research*, 9, pp.91-95.